EPJ Web of Conferences **112**, 01019 (2016)
DOI: 10.1051/epjconf/201611201019

Overview of HERMES results

Charlotte Van Hulse[1,a]

[1] *University of the Basque Country – UPV/EHU, Spain.*

Abstract. The HERMES experiment has collected a wealth of deep-inelastic scattering data using the 27.6 GeV polarized lepton beam at HERA and various pure gas targets, both unpolarized and polarized. This allowed for a series of diverse and unique measurements. Among them are measurements that provide information on the three-dimensional structure of the nucleon, both in momentum space and in position space. Results of measurements of exclusive ω production on an unpolarized and transversely polarized nucleon target, sensitive to the distribution in transverse-position and longitudinal-momentum space, are discussed as well as the three-dimensional extraction of azimuthal asymmetries measured in semi-inclusive deep-inelastic scattering, sensitive to twist-2 and twist-3 distributions in three-dimensional momentum space.

1 Introduction

The HERMES experiment was a fixed-target experiment located around the HERA accelerator at DESY in Hamburg (Germany). It took data from 1995 until 2007 by scattering longitudinally polarized electrons or positrons off a stationary gas target, internal to the beam pipe. The various types of targets used include hydrogen, deuterium, helium and heavier targets, with hydrogen longitudinally or transversely polarized or unpolarized, deuterium and helium longitudinally polarized or unpolarized, and the heavier targets unpolarized. The scattered lepton and particles produced in the collision were detected by a forward spectrometer. Here tracking was performed using multi-wire proportional chambers, while lepton-hadron particle identification was obtained using a preshower hodoscope, a calorimeter, and a transition-radiation detector, and hadron discrimination into pions, kaons and protons was achieved using a ring-imaging Cherenkov detector. The last two years of data collection got complemented by the installation of a recoil detector, located around the target, in order to detect low-energetic particles, outside of the acceptance of the forward spectrometer.

In the here presented proceedings, the focus is placed on the three-dimensional structures of the nucleon. In section 2 results sensitive to the distribution of quarks as a function of their longitudinal momentum fraction with respect to the momentum of the nucleon, where longitudinal refers to the direction of the probe used to investigate the nucleon, and their transverse position are presented. More in particular, measurements of exclusive ω production on transversely polarized and unpolarized hydrogen as well as on unpolarized deuterium are discussed.

In section 3, measurements of asymmetries that provide access to the three-dimensional structure of the nucleon in terms of the distribution of quarks as a function of their longitudinal momentum frac-

[a] e-mail: cvhulse@mail.desy.de

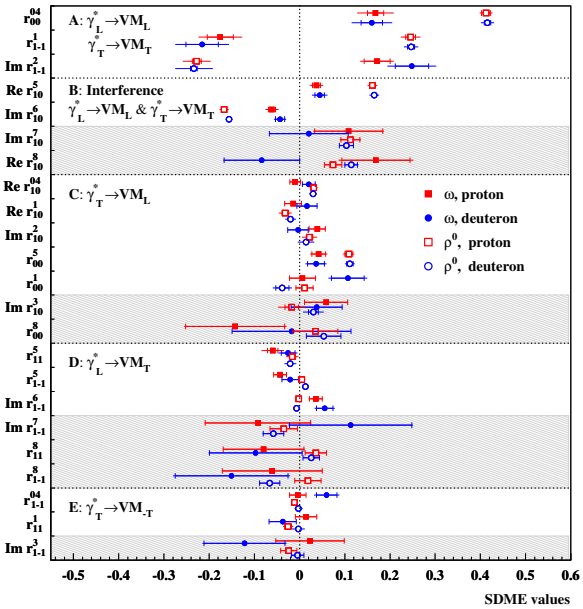

Figure 1. Extracted ω SDMEs (closed symbols) and ρ SDMEs (open symbols) for data collection on proton (red squares) and deuteron (blue circles) in the entire kinematic range. The unpolarized SDMEs are represented in the white bands, while the polarized SDMEs are represented in the grey bands. The different classes of SDMEs are labeled in the figure.

tion and transverse momentum are presented. The focus lies here on the three-dimensional extraction of the relevant asymmetry amplitudes, previously extracted one-dimensionally.

2 Exclusive ω production

The study of exclusive ω production is sensitive to generalized parton distributions (GPDs) and thus offers a means to study the three-dimensional structure of the nucleon. The Fourier transform in impact-parameter space of GPDs provides information on the distribution of quarks inside the nucleon as a function of their longitudinal momentum fraction and their transverse position. In addition, through the Ji relation, GPDs offer access to the total angular momentum of the quarks [1]. Here, the two relevant GPDs are the GPDs H and E, which both describe the distribution with parton-helicity conservation and with respectively nucleon-helicity conservation and nucleon-helicity flip. Exclusive ω production is sensitive to both these GPDs. However, for exclusive ω production on an unpolarized nucleon, the contribution of the GPD E is suppressed, and one is mainly sensitive to the GPD H. In contrast, exclusive ω production on a transversely polarized nucleon is sensitive to the interference of the GPDs H and E, thus opening access to the GPD E. In the following results on exclusive ω

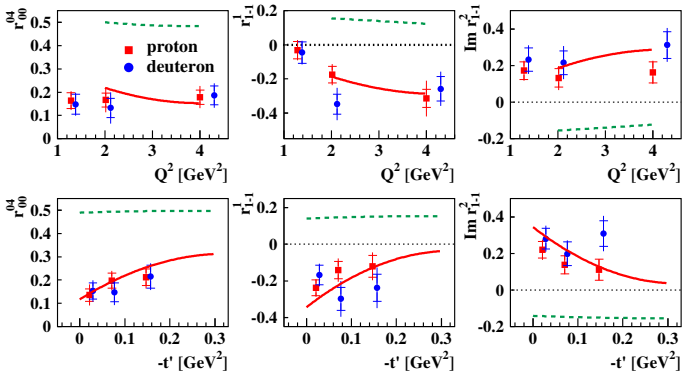

Figure 2. The class-A ω SDMEs as a function of Q^2 (upper row) and $-t'$ (lower row). The predictions of the GK model are also represented, with (red, full line) and without (green, dashed line) the pion-pole contribution.

production off unpolarized protons and deuterons as well as off transversely polarized protons are presented.

The analysis of exclusive ω production off unpolarized hydrogen and deuterium is performed through the study of the three-dimensional angular distribution of the ω-meson decay products. The ω meson decays with a branching ratio of 89.1% as $\omega \to \pi^+\pi^-\pi^0$, with $\pi^0 \to \gamma\gamma$. The angular distribution of the decay products is parametrized in terms of spin density matrix elements (SDMEs). The SDMEs themselves can be written in terms of helicity amplitudes that describe the transition of the helicity states of the initial nucleon and the virtual photon, mediating the lepton-nucleon interaction, to the helicity states of the final-state nucleon and the produced ω meson. The selection of exclusive ω production is performed using a missing-mass technique without the detection of the recoiling nucleon and the SDMEs are extracted through a maximum-likelihood fit to the angular distribution of the ω-meson decay products. For an unpolarized lepton beam fifteen "unpolarized" SDMEs are extracted and for a longitudinally polarized lepton beam eight "polarized" SDMEs are extracted.

The extracted SDMEs are presented in figure 1 for the entire kinematic range [2], in comparison with the SDMEs extracted from the exclusive production of ρ mesons [3], as measured by the HERMES collaboration as well. There are five classes of SDMEs, corresponding to the transition of a longitudinally (transversely) polarized photon to a longitudinally (transversely) polarized meson (class A), the interference of both transitions (class B), the transition of a transversely polarized photon to a longitudinally polarized meson (class C), the transition of a longitudinally polarized photon to a transversely polarized meson (class D), and finally the transition of a transversely polarized photon to a transversely polarized meson with helicity flip (class E). The conservation of s-channel helicity, i.e., the property that the photon and meson have the same helicity state, is observed for classes A and B, while for classes C and D a slight s-channel-helicity violation is observed at the 2-to-3 σ level for proton and deuteron. One can also see that the ω SDMEs r^1_{1-1} and $\Im r^2_{1-1}$ are respectively negative and positive and opposite in sign to the corresponding ρ SDMEs. This corresponds to a large unnatural-parity exchange for the ω meson and a large natural-parity exchange for the ρ meson. The term (un)natural-parity exchange refers to the quantum numbers of the particle exchanged between the virtual photon, which dissociates into a quark-antiquark pair, and the nucleon in Regge theory. In Regge phenomenology the interaction of the quark-antiquark pair with the nucleon proceeds through

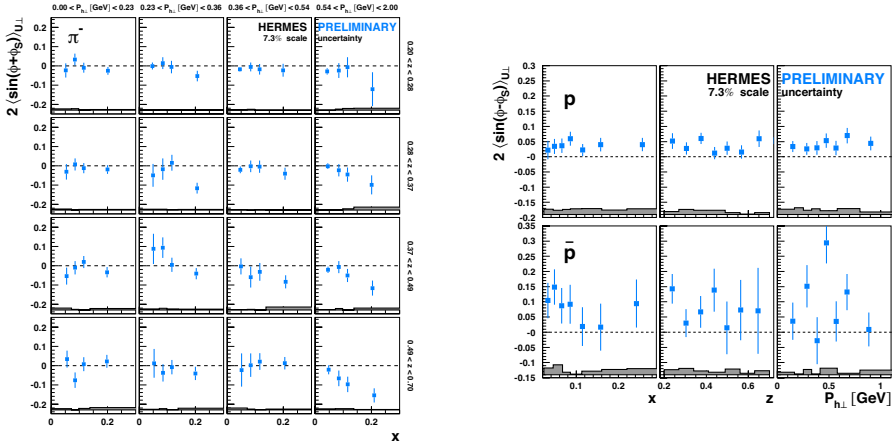

Figure 3. The Collins amplitude (left) for negative pions as a function of x for different bins in z (subdivision in rows) and $P_{h\perp}$ (subdivision in columns) and the Sivers amplitude (right) for protons and anti-protons as a function of x, z and $P_{h\perp}$.

the exchange of a pomeron or other reggeons, and depending on the quantum numbers of the particle, one talks about natural-parity exchange ($J^P = 0^+, 1^-$,..) or unnatural-parity exchange ($J^P = 0^-, 1^+$). The same large unnatural-parity exchange for ω mesons is also clearly visible from the analysis of linear combinations of specific SDMEs [3].

The extraction of the SDMEs was also performed in three kinematic bins in Q^2 and $-t'$, where $-Q^2$ represents the squared four-momentum of the virtual photon and $t' = t - t_{min}$, with t the Mandelstam variable and $-t_{min}$ the smallest kinematically allowed value of $-t$ at fixed virtual-photon energy and Q^2. As an example, the measurements for the class-A SDMEs are shown in figure 2. No pronounced kinematic dependence is observed, neither for class A nor for the other classes. Also shown in the figure are the results of the calculations from the "GK" model [4]. Two versions of the model are shown: one including the full contribution to the electromagnetic form factor from the pion (full, red line) and one taking only into account the relatively small perturbative contribution to this form factor (green, dashed line). As can be seen, the inclusion of the pion pole results in good agreement between the experimental data and the model.

From the data collected on transversely polarized protons, five sine and two cosine asymmetry amplitudes were extracted in the entire kinematic range as well as in two bins of Q^2 and $-t'$ [5]. Within the GK model, the experimental data favours the version of the model with pion-pole contribution with a positive $\pi\omega$ transition form factor above the versions without pion-pole contribution and with pion-pole contribution with a negative $\pi\omega$ transition form factor.

3 Asymmetries in semi-inclusive deep-inelastic scattering

Semi-inclusive deep-inelastic scattering (DIS) offers the possibility to study the three-dimensional distribution of the nucleon in terms of transverse-momentum-dependent (TMD) parton distribution functions (PDFs). These describe the distribution of partons as a function of their longitudinal and

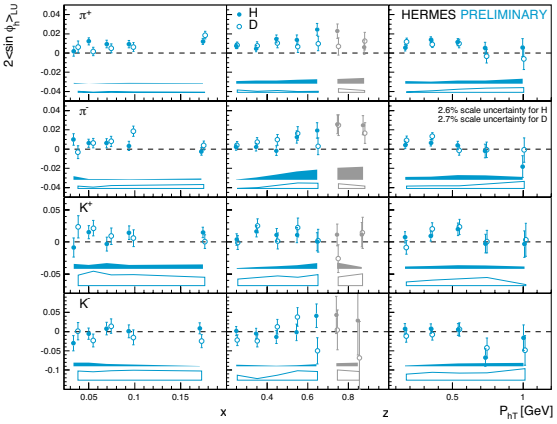

Figure 4. Lepton-beam asymmetries for pions (upper two rows) and kaons (lower two rows) as a function of x, z and $P_{h\perp}$ (labeled as P_{hT}). Note that for the projections in x and $P_{h\perp}$, the highest two z bins, indicated in grey, are not included.

transverse momenta. At leading-twist, eight TMD PDFs are needed to describe the full semi-inclusive DIS cross section, each of them relating to a specific spin-state configuration of the quark and the nucleon. For example, the Sivers TMD PDF describes the distribution of unpolarized quarks in a transversely polarized nucleon, the transversity distribution describes the distribution of transversely polarized quarks in a transversely polarized nucleon and the Boer-Mulders distribution describes the distribution of transversely polarized quarks in an unpolarized nucleon. The TMD PDFs enter the cross section in convolution with a fragmentation function, which describes the fragmentation of a quark into a final-state hadron. The two fragmentation functions of relevance are the spin-independent fragmentation function and the Collins fragmentation function, which describes the fragmentation of a transversely polarized quark into an unpolarized hadron. The TMD PDF, in combination with the fragmentation function, can be accessed through the extraction of asymmetries, given that each combination enters the cross section with a characteristic angular modulation. Besides the leading-twist contributions, also higher-twist contributions enter the cross section.

The one-dimensional extraction for pions and kaons of the Collins amplitude, sensitive to the transversity distribution and the Collins fragmentation function, and of the Sivers amplitude, sensitive to the Sivers PDF and the spin-independent fragmentation function, had been performed previously by the HERMES collaboration as a function of x, z and $P_{h\perp}$ using data collected on a transversely polarized hydrogen target [6–8]. Here, x represents the Bjorken-x variable, z the fractional energy of the produced hadron with respect to the virtual-photon energy and $P_{h\perp}$ the transverse momentum of the produced hadron. The analysis has been extended by performing a three-dimensional extraction of all amplitudes related to a transversely polarized target and including also results for protons and anti-protons, where for the latter due to limited statistics only a one-dimensional extraction was possible.

In figure 3, left, the Collins amplitude is shown for negative pions as a function of x for different bins in z (subdivision in rows) and $P_{h\perp}$ (subdivision in columns). The asymmetry amplitude is on average negative. In the one-dimensional extraction, a rise of the magnitude of the asymmetry amplitude

with increasing x is observed. In the present three-dimensional extraction, this rise is seen to be concentrated at high values of $P_{h\perp}$. For positive pions, an analogous behaviour in the three-dimensional extraction is not clearly observed, although in the one-dimensional extraction a rise of the asymmetry amplitude, which on average is positive in sign, with increasing x is also seen.

In figure 3, right, the one-dimensional extraction of the Sivers amplitude is shown for protons and anti-protons as a function of x, z and $P_{h\perp}$. The data for the anti-protons is clearly limited by statistics, while the protons show a clear positive asymmetry amplitude, without a clear dependence on any of the kinematic variables. For protons, also the three-dimensional extraction was performed. From this extraction, no clear dependence on any of the kinematic variables is observed neither.

As stated earlier, besides the leading-twist contributions, also higher-twist contributions enter the cross section. Among those extracted, the twist-3 contribution to the cross section for longitudinally polarized beam and unpolarized nucleon is discussed here. This twist-3 contribution is sensitive to a combination of twist-3 PDFs, e and $g^{\perp}$, and twist-2 fragmentation functions, the Collins and spin-independent fragmentation functions, and a combination of twist-2 PDFs, the spin-independent PDF and the Boer-Mulders PDF, and twist-3 fragmentation functions, $\tilde{G}^{\perp}$ and $\tilde{E}$ [9]. The extraction of the twist-3 contribution has been performed one- and three-dimensionally in x, z and $P_{h\perp}$ for pions, kaons and protons for data collected on a hydrogen and deuterium target. In figure 4, the asymmetries extracted in one dimension as a function of x, z and $P_{h\perp}$ are shown for pions and kaons. Note that the projections in x and $P_{h\perp}$ only contain the z region of $z < 0.7$. The asymmetries for pions are positive. They increase with increasing z up to z of 0.7 and decrease with increasing $P_{h\perp}$. Also the positive kaons show a positive asymmetry amplitude, but no specific kinematic dependence is observed. The asymmetries for negative kaons are consistent with zero. The same observation is true for protons and anti-protons.

References

[1] X. Ji, Phys. Rev. Lett. **78**, 610 (1997).
[2] A. Airapetian et al., Eur. Phys. J. C **74**, 3110 (2014).
[3] A. Airapetian et al., Eur. Phys. J. C **62**, 659 (2009).
[4] S. Goloskokov and P. Kroll, Eur. Phys. J **A** 50, 146 (2014).
[5] A. Airapetian et al., Eur. Phys. J. C **75**, 600 (2015).
[6] A. Airapetian et al., Phys. Rev. Lett. **94**, 012002 (2005).
[7] A. Airapetian et al., Phys. Lett. B **693**, 11-16 (2010).
[8] A. Airapetian et al., Phys. Rev. Lett. **103**, 152002 (2009).
[9] A. Bacchetta et al., JHEP **0702**, 093 (2007).